Journal of Alloys and Compounds, 186 (1992) 361–367
JALCOM 288

Analysis of $YBa_2Cu_3O_{7-\delta}$ crystal growth from $BaCO_3$–CuO–Y_2O_3 charges

P. Diko, A. Kasardova, J. Miskuf and K. Csach
Institute of Experimental Physics, Slovak Academy of Sciences, Solovjevova 47, 04353 Kosice (Czechoslovakia)

(Received February 28, 1992)

Abstract

Crystal growth from incompletely melted charges with starting compositions $BaCO_3 + CuO + Y_2O_3$ in air has been studied. The solid melt and all crystals in the caverns were analysed. The reaction $BaCO_3 + CuO \rightarrow BaCuO_2 + CO_2$ was found to control the melting and crystallization. Changes in the melt during the process led to CuO, Y_2BaCuO_5, $YBa_2Cu_3O_{7-\delta}$ and $BaCuO_2$ primary crystallization. Different CuO and Cu_2O crystallization forms were found.

1. Introduction

Thin $YBa_2Cu_3O_{7-\delta}$ single crystals have often been prepared from incompletely melted charges. In many cases single crystals of sufficient dimensions were obtained in spite of rather different temperature regimes and starting compositions [1–7]. The maximum dwell temperatures for melting ranged from 1000 to 1400 °C with different dwell times and cooling rates. Calcined or uncalcined mixtures of $BaCO_3$, CuO and Y_2O_3 were used. These single crystals were found to be contaminated by crucible materials to a greater or lesser extent depending on the temperature regime of crystal growth.

Thicker single crystals have been prepared from homogeneous melts [8–11]. Unfortunately, owing to partial dissolution of the crucibles during melting and the very low cooling rates used, serious problems of impurity contamination were encountered.

The aim of this work is to study the conditions of $YBa_2Cu_3O_{7-\delta}$ single-crystal growth from unhomogenized melts by analysing the products of crystal growth from different starting compositions and in different temperature regimes.

2. Experimental procedure

We have carried out our experiments with three different starting compositions chosen from the usual range of compositions employed (Table 1).

0925-8388/92/$5.00

TABLE 1

Results of crystal analysis

Starting composition $YO_{1.5}$:BaO:CuO (at.%)	Temperature (°C)	Grown crystals	Dimensions of 123 crystals (mm^3)
2:29.5:68.5	995	123 thin plates, 211 needles, 011 thick plates	0.4×0.4×0.02
	1040	123 thin plates, 011 thick plates, 001 needle crystals	1×1×0.03
	1085	123 thin plates, 011 thick plates, 001 needle crystals	3×3×0.03
4:27.5:68.5	995	123 thin plates, 211 needles, 011 thick plates	1×1×0.05
	1040	123 thin plates, 211 needles, 001 needle crystals, 011 thick plates	2×2×0.03
	1085	123 thin plates, 211 needles, 011 thick plates, 001 needles, 001 dendrites	1×1×0.04
5:32:63	1040	123 thin plates, 011 thick plates, 001 spheres, 001 crystals	0.2×0.2×0.03
	1085	211 needle crystals, 011 thick plates, 123 thin plates, 001 dendrites, 001 crystals	0.1×0.1×0.03
	1110	211 needle crystals, 011 thick plates, 123 thin plates, 001 crystals, 001 dendrites	0.3×0.2×0.02

Y_2O_3, $BaCO_3$ and CuO powders of 99.99% minimum purity (Merck) were mixed and ground in an agate mortar using ethanol. The charges were lightly pressed into the crucibles. In all cases we used alumina crucibles 24 mm in diameter and height. The crystal growth processes were realized in an Adamel Lomargy tubular furnace with a temperature programmer in air. Temperature regimes were as follows: heating from room temperature to dwell temperature (Table 1) at a heating rate of 13 °C min^{-1}, dwell for 1 h, slow cooling at a cooling rate of 6 °C h^{-1} to 840 °C and then cooling with the furnace to room temperature.

After the crystal growth experiments the crucibles were crushed and the crystals were separated. Metallographic samples were prepared from the solid melts and their microstructure was studied by light microscopy. Phases and crystals were defined by energy-dispersive X-ray (EDX) analysis in a raster electron microscope.

3. Experimental results

At all our dwell temperatures the melting of charges was only partial. The amount of melt on the bottom of the crucible increased with increasing

dwell temperature. Above the melt the rest of the charge was sintered. Single crystals grew in the caverns as usual.

Metallographic analyses of the solid melts showed multiphase structures. Besides eutectic $CuO + BaCuO_2$ with a small content of yttrium (Fig. 1), we also observed white copper oxide, grey $BaCuO_2$ phase and dark globular particles in which only barium was detected by EDX analysis (Fig. 2). We have established by X-ray analysis that these particles are unreacted $BaCO_3$.

The results of the electron microscopy observations and EDX analyses of all types of crystals found in the caverns are summarized in Table 1. It is seen from the table that besides $YBa_2Cu_3O_{7-\delta}$ (123) crystals, Y_2BaCuO_5 (211), $BaCuO_2$ (011) and copper oxide (001) were also detected. The sizes and amounts of 123 single crystals were influenced by the applied temperature regime and starting composition. Small crystals were usually accompanied by copper oxide (Fig. 3) and 011 phase (Fig. 4). Often we could see flux enclosed by growing 123 single crystals (Fig. 5). Crystals were larger at higher dwell temperature and with lower $YO_{1.5}$ content. The greatest number

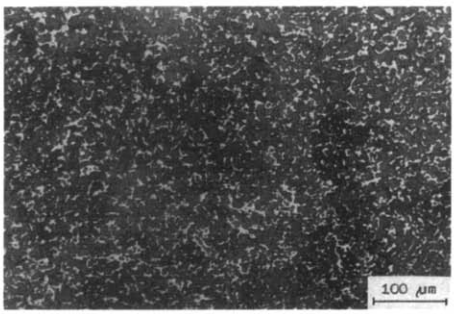

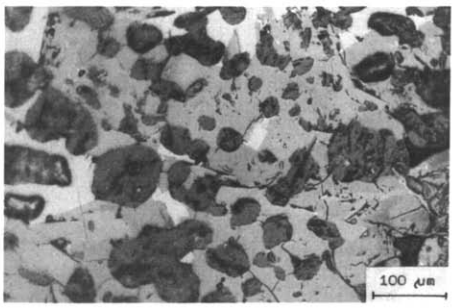

Fig. 1. Normal light micrograph of CuO (light phase) + $BaCuO_2$ (dark phase) eutectic (5:32:63 charge, 1040 °C).

Fig. 2. Normal light micrograph showing white copper oxide, grey $BaCuO_2$ and dark $BaCO_3$ phases (5:32:63 charge, 1040 °C).

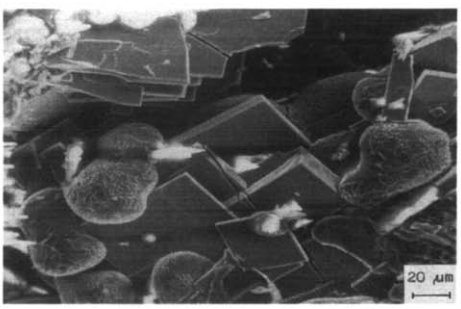

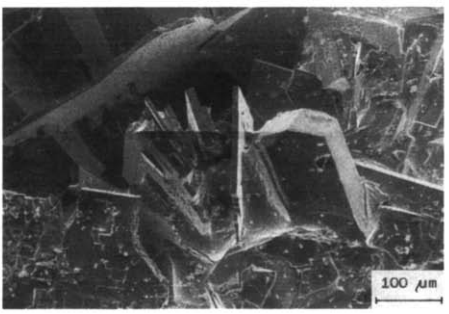

Fig. 3. SEM image of small $YBa_2Cu_3O_{7-\delta}$ crystals, copper oxide in near-globular form and bright $BaCO_3$ particles (5:32:63 charge, 1040 °C).

Fig. 4. SEM image of thin $YBa_2Cu_3O_{7-\delta}$ crystals and thick $BaCuO_2$ crystal (4:27.5:68.5 charge, 995 °C).

of large crystals was obtained from the starting composition $YO_{1.5}$:BaO:CuO = 2:29.5:68.5 after dwell at 1040 °C. These crystals reached maximum dimensions of 2–3 mm in the "*ab*" plane (Fig. 6). The thickness of all crystals was not much influenced by the starting chemical composition or by the dwell temperature and was in the range 20–50 μm. The content of aluminium (crucible contamination) in the 123 crystals was below the detection limit of the EDX analyser.

In the case of compositions with a higher content of $YO_{1.5}$, 211 crystals of considerable dimensions and of needle-like shape with sharp edges grew. The largest 211 crystals were obtained from the starting composition $YO_{1.5}$:BaO:CuO = 5:32:63 and after dwell at 1095 °C (Fig. 7). In all charges large 001 crystals of elongated form and with oval edges were present (Fig. 8). It was interesting that at all dwell temperatures above 1026 °C we observed copper oxide in two morphological forms. Besides well-shaped crystals, a form of more or less developed dendrites of copper oxide was found (Figs. 3 and 9). The 011 phase was present in all samples as single crystals (Fig. 4) or aggregates (Fig. 10). As on the metallographic cuts, bright particles of unreacted $BaCO_3$ were observed in the caverns (Figs. 3 and 9).

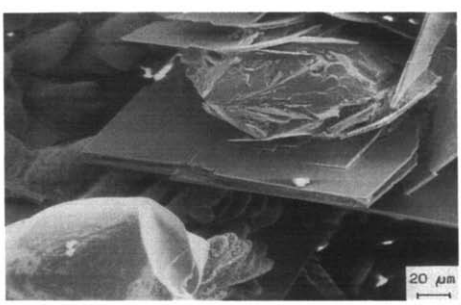

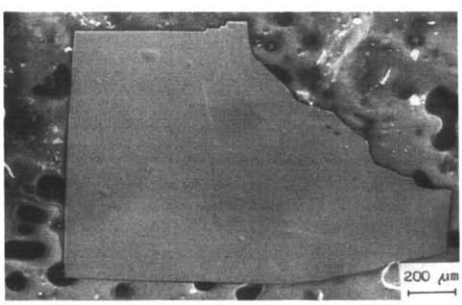

Fig. 5. SEM image of flux-enclosed growing $YBa_2Cu_3O_{7-\delta}$ crystal (5:32:63 charge, 1085 °C).

Fig. 6. SEM image of large $YBa_2Cu_3O_{7-\delta}$ single crystal, "*ab*" surface (2:29.5:68.5 charge, 1040 °C).

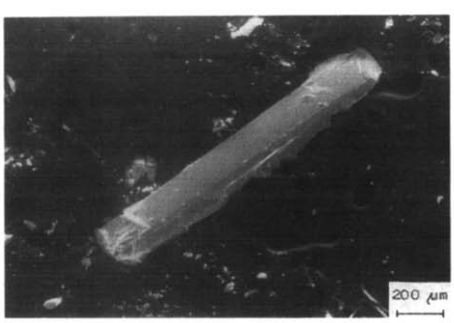

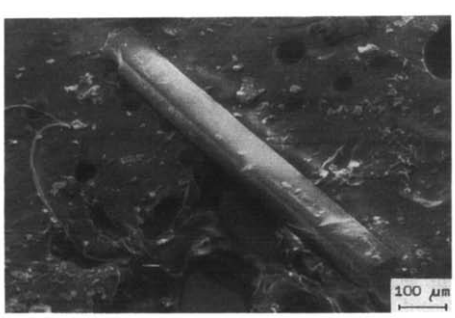

Fig. 7. SEM image of Y_2BaCuO_5 single crystal with sharp edges (5:32:63 charge, 1085 °C).

Fig. 8. SEM image of CuO crystal with oval edges (2:29.5:68.5 charge, 1040 °C).

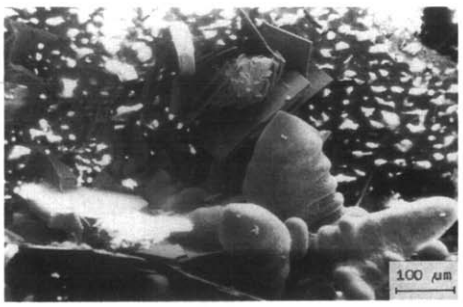

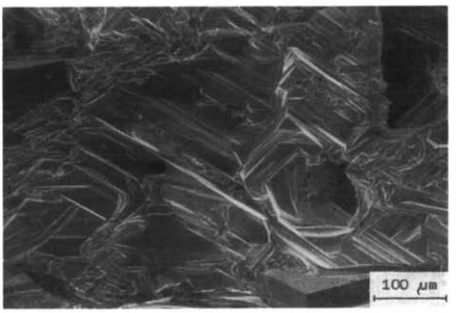

Fig. 9. SEM image of dendritic form of copper oxide, thin $YBa_2Cu_3O_{7-\delta}$ plates and bright $BaCO_3$ particles (5:32:63 charge, 1085 °C).

Fig. 10. SEM image of $BaCuO_2$ aggregates (2:29.5:68.5 charge, 995 °C).

4. Discussion

From the metallographic and EDX analyses it follows that $BaCO_3$ was not wholly decomposed. This means that the crystal growth was realized in the presence of residual $BaCO_3$ and from a non-equilibrium melt. In such a case it is necessary to take into account not only the thermodynamic equilibrium states, but also the kinetics of ongoing reactions and the segregation of components formed on partial melting. Working with the starting composition $BaCO_3 + CuO + YO_{1.5}$, it is necessary to consider the following consecutive reactions in the solid state [12]:

$$BaCO_3 + CuO \longrightarrow BaCuO_2 + CO_2 \quad (1)$$

$$BaCuO_2 + Y_2O_3 \longrightarrow Y_2BaCuO_5 \quad (2)$$

$$Y_2BaCuO_5 + 3BaCuO_2 + 2CuO \longrightarrow 2YBa_2Cu_3O_{6.5-x} + xO_2 \quad (3)$$

The following reactions taking place at the invariant points are the main ones resulting in melt (L) formation [13]:

$$YBa_2Cu_3O_x + BaCuO_2 + CuO \longrightarrow L \quad (890\ °C) \quad (4)$$

$$BaCuO_2 + CuO \longrightarrow L \quad (920\ °C) \quad (5)$$

$$Y_2BaCuO_5 + BaCuO_2 \longrightarrow L \quad (1000\ °C) \quad (6)$$

$$BaCuO_2 \longrightarrow L \quad (1015\ °C) \quad (7)$$

$$CuO \longrightarrow Cu_2O \quad (1026\ °C) \quad (8)$$

Since the metallographic and EDX analyses showed that unreacted $BaCO_3$ was present in the charges after the crystal growth process, this means that reaction (1) controls the melting and crystal growth. On the basis of these reactions we can consider that the first melt is formed at 890 °C (reaction (4)), but taking into account the 011 and 123 amounts in the charge and the heating rate used, we cannot expect a high amount of melt at this

temperature. The basic reactions for the melting will be reactions (5)–(7). The created melt will leak to the bottom of the crucible where it will be enriched with CuO and $YO_{1.5}$ by solution of 001 and 211 phases. (A role may also be played by the difference in density between $BaCO_3$ (4.43 g cm^{-3}) and CuO (6.4 g cm^{-3}).) In this way a melt saturated with CuO and $YO_{1.5}$ is formed in the lower part of the crucible with a composition given by the liquidus surface in the ternary $YO_{1.5}+BaO+CuO$ equilibrium diagram (Fig. 11) [14]. We can assume that with increasing temperature the melt will be richer in CuO and $YO_{1.5}$ because the liquidus area is dilated. After solution of all 001 phase at the bottom of the crucible, the melt begins to be enriched with barium through $BaCuO_2$ leaking from the upper parts of the charge. With decreasing temperature copper oxides crystallize from the CuO-saturated melt in the form of Cu_2O above 1026 °C and CuO below this temperature. By gradual saturation of the melt with BaO, the composition of the melt is moved through the regions of primary crystallization of 211, 123 and finally 011 phases. Under such conditions of crystallization it is evidently possible to find suitable temperature regimes for 123 crystal growth of sufficient dimensions for a wide range of starting compositions.

An interesting observation was the presence of copper oxide in two morphological variations, *i.e.* as crystals and dendrites. Taking into account that the crystalline form was found in all charges and the dendritic form only in charges at a dwell temperature above 1026 °C, we can say that copper oxide crystallized in the dendritic form as Cu_2O.

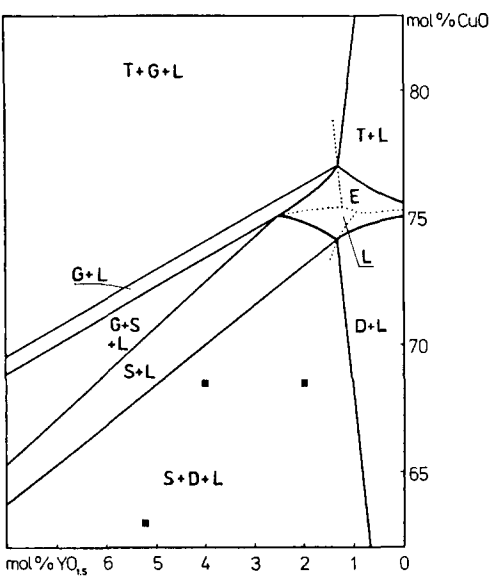

Fig. 11. Isothermal section of the system Y–Ba–Cu–O–(O) in air at 950 °C. Projections of primary crystallization field boundaries are denoted by dotted lines. Capital letters denote phases: S, $YBa_2Cu_3O_{7-\delta}$; D, $BaCuO_2$; G, Y_2BaCuO_5; T, CuO; L, melt [14]. Full squares denote results from our growth experiments.

5. Conclusions

We have shown that in the case of a $BaCO_3 + CuO$ flux the melting and crystal growth are controlled by the reaction $BaCO_3 + CuO \rightarrow BaCuO_2 + CO_2$. For higher heating rates and short dwell times at the maximum temperature, only part of the charge is melted and, as we have discussed, the composition of the melt continuously changes from CuO and $YO_{1.5}$ rich to BaO rich. Under such conditions Cu_2O, CuO, Y_2BaCuO_5, $YBa_2Cu_3O_{7-\delta}$ and $BaCuO_2$ phases can crystallize as primary phases from the melt. Thus it is possible to find optimum temperature regimes for $YBa_2Cu_3O_{7-\delta}$ crystal growth for a wide region of starting compositions. It is possible to obtain lowly contaminated single crystals from alumina crucibles.

We have found conditions for the growth of quite large Y_2BaCuO_5 crystals. Crystallization of copper oxide in dendritic (Cu_2O) and crystalline (CuO) variations was observed.

References

1 K. L. Keester, R. M. Houstley and D. B. Marshall, *J. Magn. Magn. Mater., 76–77* (1988) 626.
2 J. A. Campa and J. M. Gomez de Salazar, *J. Cryst. Growth, 91* (1988) 334.
3 A. B. Bykov, L. N. Demianets, I. P. Zibrov, K. V. Kanunnits, O. K. Melnikov and S. M. Tishov, *J. Cryst. Growth, 91* (1988) 295.
4 N. V. Ch. Shekar, J. Suresh, K. Govinda Rajan and G. V. N. Rao, *Bull. Mater. Sci., 11* (1988) 277.
5 A. Ono, H. Nozaky and Y. Ishizava, *Jpn. J. Appl. Phys., 27* (1988) L340.
6 H. Katayama-Yoshida, I. Okabe, T. Takahashi, T. Sasaki, T. Hirooka, T. Suzuki, T. Ciszek and K. Deb, *Jpn. J. Appl. Phys., 26* (1987) L2007.
7 D. L. Kaiser, F. Holtzberg, M. F. Chisholm and T. K. Worthington, *J. Cryst. Growth, 85* (1987) 593.
8 M. Newriva, P. Holba, S. Durcok, D. Zemanova, E. Polert and A. Triska, *Physica C, 157* (1989) 334.
9 Th. Wolf, W. Goldacker, B. Obst, G. Roth and R. Flukinger, *J. Cryst. Growth, 96* (1989) 1010.
10 K. Watanabe, *J. Cryst. Growth, 100* (1990) 293.
11 H. J. Scheel and F. Licci, *MRS Bull.*, (10) (1988) 56.
12 A. M. Gadalla and T. Hegg, *Thermochim. Acta, 145* (1989) 149.
13 T. Aselage and K. Keefer, *J. Mater. Res., 3* (1988) 1279.
14 M. Nevriva, E. Polert, J. Hejtmanek, S. Durcok, M. Simeckova and P. Diko, *Physica C, 139* (1991) 253.